ELSEVIER

Tectonophysics 356 (2002) 181–197

TECTONOPHYSICS

www.elsevier.com/locate/tecto

Moment tensors and micromechanical models

James F. Hazzard*, R. Paul Young [1]

Applied Seismology Laboratory, Department of Earth Sciences, University of Liverpool, 4 Brownlow Street, Liverpool, L69 7GP, UK

Received 23 October 2001; accepted 21 February 2002

Abstract

A numerical modelling approach that simulates cracking and failure in rock and the associated seismicity is presented and a technique is described for quantifying the seismic source mechanisms of the modelled events. The modelling approach represents rock as an assemblage of circular particles bonded together at points of contact. The connecting bonds can break under applied stress forming cracks and fractures in the modelled rock. If numerical damping is set to reproduce realistic levels of attenuation, then energy is released when the bonds break and seismic source information can be obtained as damage occurs. A technique is described by which moment tensors and moment magnitudes can be calculated for these simulated seismic events. The technique basically involves integrating around the source and summing the components of force change at the surrounding particle contacts to obtain the elements of the moment tensor matrix. The moment magnitude is then calculated from the eigenvalues of the moment tensor. The modelling approach is tested by simulating a well-controlled experiment in which a tunnel is excavated in highly stressed granite while microseismicity is recorded. The seismicity produced by the model is compared to the actual recorded seismicity underground. The model reproduces the spatial and temporal distribution of seismicity observed around the tunnel and also the magnitudes of the events. A direct comparison between the actual and simulated moment tensors is not performed due to the two-dimensional nature of the model, however, qualitative comparisons are presented and it is shown that the model produces intuitively realistic source mechanisms. The ability to obtain seismic source information from the models provides a unique means for model validation through comparison with actual recorded seismicity. Once it is established that the model is performing in a realistic manner, it can then be used to examine the micromechanics of cracking, failure and the associated seismicity and to help resolve the non-uniqueness of the geophysical interpretation. This is demonstrated by examining in detail the mechanics of one of the modelled seismic events by observation of the time dependence of the moment tensor and by direct examination of the particle motions at the simulated source.

Keywords: Micromechanics; PFC; Moment tensor; Dynamic model

1. Introduction

With increasing computer power, discontinuum modelling techniques are becoming an increasingly popular way to study rock deformation processes. In these models, individual elements move independently of one another and interact only at points of contact. Antonellini and Pollard (1995) and Morgan

* Corresponding author. Tel.: +44-151-794-5160; fax: +44-151-794-5169.

E-mail addresses: hazzard@liv.ac.uk (J.F. Hazzard), r.p.young@liv.ac.uk (R.P. Young).

[1] Tel.: +44-151-794-5178; fax: +44-151-794-5169.

0040-1951/02/$ - see front matter © 2002 Elsevier Science B.V. All rights reserved.
PII: S0040-1951(02)00384-0

and Boettcher (1999) use particle models to simulate deformation bands in shear zones. Mora and Place (1998) take this a step further by modelling tectonic scale earthquakes with gouge. Cracking and fracture in intact rocks can be simulated by bonding together individual elements (particles) and observing bond breakages as stress is applied (see Potyondy and Autio, 2001). These models possess the advantage that no a priori assumptions need to be made about where and how fracture and failure will occur—cracking can occur spontaneously and can exhibit a variety of mechanisms when certain local stress conditions are exceeded. This attribute of the models suggests that interesting insights into the mechanics of deformation and failure under different stress conditions could be obtained if the failure mechanisms produced by the models could be quantified and studied. This is the purpose of the research presented here.

It is possible to run these bonded particle models dynamically with low numerical damping such that energy is released when bonds break (see Hazzard et al., 2000). In this way, bond breakages can be considered seismic events and the strength of the events can be quantified by observing the amount of energy release (Hazzard and Young, 2000). It was thought that this approach could be extended and that the mechanics of the simulated seismic sources could be determined to yield interesting information about the nature of cracking, deformation and failure. The ability to quantify the nature and strength of the seismic source could also provide a unique way to validate the models by comparing the modelled seismicity to actual seismic source information for events recorded in the laboratory or field.

A well-known method for quantification of the mechanics of a seismic source is through calculation of the moment tensor (see Aki and Richards, 1980). The moment tensor is a representation of a seismic source by a set of equivalent forces that produce the same displacements at the earth's surface as the actual forces active at the source. The moment tensor is calculated in the field by recording waveforms and minimising the misfit between a set of model predictions and a set of observed responses. The same indirect technique could be used in the dynamic bonded-particle models to calculate moment tensors. However, since all particle positions, forces and motions are known in the models, it was thought that a more efficient, direct approach could be used. A possible direct technique for calculating moment tensors in these dynamic bonded-particle models is presented here.

The technique is tested by simulating an underground excavation in highly stressed granite in which microseismicity was recorded during the excavation (Chandler et al., 2000). The locations, magnitudes and moment tensors of the seismic events produced by the model are compared with the actual seismic information determined from the field study. As well as providing a means to assess the accuracy of the modelling technique, the excavation model is also used to investigate in detail the micromechanics of failure around the tunnel by examining the time dependence of the moment tensors and by direct observation of the particle motions during a seismic event. In this way, the model can provide added information not available from the seismic data and can help resolve the non-uniqueness of the geophysical interpretation.

2. Modelling approach

2.1. Particle flow code

Models are generated using the commercially available Particle Flow Code in 2 Dimensions or PFC^{2D} (Itasca Consulting Group, 1999). With this software, a two-dimensional slice of rock is modelled as a random assembly of distinct round particles (disks) bonded together at points of contact. The particle contacts are assigned a normal and shear stiffness and these micro stiffnesses influence the macro deformation properties of the modelled rock (Young's modulus and Poisson's ratio). The connecting bonds are assigned a tensile and shear strength and these micro strengths, together with the contact stiffnesses, dictate the macro strength of the rock and the nature of failure. In addition, interparticle friction can be specified and this parameter influences the post-failure behaviour of the modelled rock.

By adjusting the micro particle parameters, realistic macromechanical rock behaviour can be reproduced. This approach allows for rock damage to be simulated directly on the micromechanical scale so that there is

no need to include complicated constitutive relationships as in continuum modelling. This technique also allows for examination of the cracking and damage patterns occurring on the micro scale during deformation experiments (see Potyondy et al., 1996; Hazzard et al., 2000 for more details of modelling rock using PFC^{2D}).

As well as enabling the direct examination of cracking and failure, PFC can also be run dynamically such that waves propagate out from the induced fractures. PFC uses the distinct element approach to model the forces and motions of the particles within the assembly (Cundall and Strack, 1979). This method is similar to that used in explicit finite-difference analyses and allows information to propagate dynamically through the system. For this reason, PFC^{2D} is a logical choice for modelling seismicity and the resulting dynamic output.

2.2. Modelling seismicity

2.2.1. General considerations

When stress is applied to the model, strain energy is stored at the particle contacts. If local stresses are high enough, bonds connecting the particles may break. When this happens, the previously bonded particles move rapidly apart until stopped by local confinement. The stored strain energy is then converted into heat (due to inter particle friction), energy absorbed by numerical damping, increased strain energy in neighbouring contacts and kinetic energy. By adjusting the numerical damping, realistic levels of attenuation can be simulated and realistic levels of kinetic energy release can be observed (Hazzard et al., 2000).

Previous research has used particle models to simulate seismicity. Mora and Place (1998) calculate stress drops for simulated stick–slip motion on a fault and Hazzard and Young (2000) calculate magnitudes of simulated acoustic emissions. However, few, if any, studies exist in which source mechanisms are examined and moment tensors are calculated.

In some respects, it would appear unnecessary to try to calculate moment tensors for modelled events since a moment tensor is itself an idealised model of a source. The moment tensor calculation generally assumes a point source in space and time. This is unlikely to be the case, especially in a model composed of discrete elements of finite size. However, it is proposed that the moment tensor representation provides a useful way to quantify the nature of the modelled events and will facilitate comparisons with actual recorded seismicity. Once the events of interest have been defined, more detailed examinations of the micromechanics can be performed by directly examining the forces and motions of the particles at the source.

2.2.2. Moment tensor calculations

There are several possible ways that moment tensors could be calculated in PFC, including recording and inverting waveforms. This is clearly not the most efficient approach since particle forces and motions can be determined directly in the model. A simple yet fairly robust technique is presented here that uses the change in contact forces around bond breakages to calculate the moment tensor.

It can be assumed that each bond breakage in PFC represents a single microcrack. When a bond breaks, the two particles on either side of the crack (the source particles) will move and contacts surrounding the source particles will suffer some deformation. There will therefore be a force change at the surrounding contacts due to the formation of the crack. We can then perform an "integration" around the contacts surrounding the crack to calculate components of the moment tensor from the contact locations and force changes. For a discrete medium, the integration is a sum so the moment tensor can be calculated by:

$$M_{ij} = \sum_{S} \Delta F_i R_j \tag{1}$$

Where ΔF_i is the ith component of the change in contact force, and R_j is jth component of the distance between the contact point and the event centroid. The sum is performed over the surface, S, enclosing the event.

The event centroid is assumed to be the location of the previously bonded contact. If more than one bond breakage makes up the event (see Section 2.2.4), then the geometrical centre of the event is used. This is not the most rigorous approach since the best point source of a seismic event is actually the centroid of the stress glut (Backus, 1977). However, tests to examine the sensitivity of the calculated moment tensor to the centroid location have shown that the geometric

centroid generally produces satisfactory results in the models.

An example event is shown in Fig. 1. This diagram depicts the situation 0.37 μs after a tensile bond breakage in a simulation of an axial loading test on a small granite core sample. The particle velocities show rapid extensional motion perpendicular to the crack (like an opening tensile crack) and the force changes at the surrounding contacts reflect this. The moment tensor calculated using Eq. (1) is shown in Fig. 1b. The moment tensor representation depicts the principal values (eigenvalues) of the moment tensor matrix as two sets of arrows whose direction and length indicate the orientation and magnitude, respectively, of the principal values. It can be seen in Fig. 1b that the event is mostly extensional with the direction of opening perpendicular to the crack orientation. There is also a small component of compression parallel to the crack. This represents the compensating motion of the particles above and below the crack moving inwards to fill the vacated space.

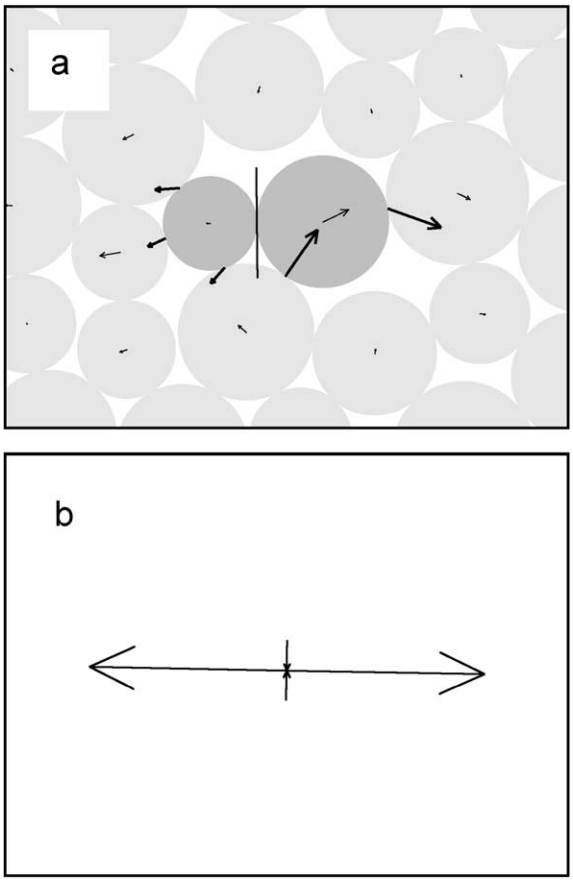

Fig. 1. An example seismic event composed of a single tensile crack. (a) Particle velocities (light arrows) and contact force changes (heavy arrows) 0.37 μs after the bond breakage. The crack is represented by a subvertical black line between the two darkened source particles. (b) The calculated moment tensor.

2.2.3. Time dependence and magnitude calculation

It is known that seismic events evolve through time and it is possible to calculate time-dependent moment tensors to reveal information about the nature of rupture initiation and propagation (Baker and Young, 1997). In the PFC model, the moment tensor can be calculated at each time step after the initial rupture and the evolution of the source type can be examined. In theory, a full time-dependent moment tensor can be obtained for each event. However, in practice, storing the full time-dependent moment tensor for all events would be very memory intensive, therefore, in general only a single moment tensor is stored for each event. For particular events of interest, the full time-dependent moment tensor could be examined along with the micromechanics of failure (see Section 3.5).

The single moment tensor that is stored for each event (the time-*independent* moment tensor) is the moment tensor calculated at the time of maximum scalar moment. The scalar moment can be calculated from the elements of the moment tensor matrix by:

$$M_0 = \left(\frac{\sum_{j=1}^{3} m_j^2}{2} \right)^{1/2} \tag{2}$$

where m_j is the jth eigenvalue of the moment tensor matrix (Silver and Jordan, 1982). Other techniques for determining the scalar moment exist (see Bowers and Hudson, 1999), however, it is thought that the differences between different methods will be small; therefore these have not been examined here.

Fig. 2 shows the calculated scalar moment plotted against time for the tensile event shown in Fig. 1. It can be seen that the moment quickly increases to some peak value and then begins to drop. In tests where the recording was continued further, the moment continued to oscillate with decreasing amplitude

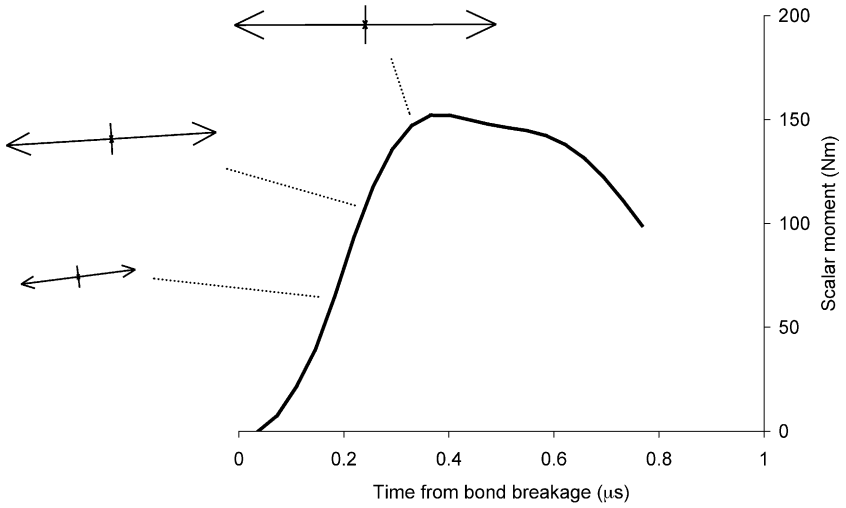

Fig. 2. Time evolution of the tensile event from Fig. 1.

until eventually a constant value slightly lower than the peak was reached. Moment tensors calculated at different times during the event are shown. The moment tensors are scaled according to the scalar moment. It is interesting to observe how the event evolves through time. As well as increasing in magnitude, there appears to be a slight rotation of the principal force directions. Time-dependent analyses for more complex events will be shown in Section 3.5.

The single time-*independent* moment tensor associated with this event is assumed to be the moment tensor calculated at the time of peak scalar moment (as shown in Fig. 1). The moment magnitude associated with the event can also be calculated from the peak scalar moment by:

$$M_w = \frac{2}{3}\log M_0 - 6 \quad (3)$$

(Hanks and Kanamori, 1979). Note that this equation is only strictly valid for events with magnitudes greater than about 3, however, it has been used with some success in other microseismic investigations (e.g. McGarr, 1994) and will also be used here. Using this equation, the magnitude of the event shown in Fig. 2 would be -4.5. Note that Hazzard and Young (2000) use the kinetic energy of the particles to calculate the event magnitude, however, this technique tends to produce magnitudes that are too large—possibly because some of the kinetic energy is not contributing to seismic motion and should be considered 'incoherent', i.e. some of the particle vibrations are combining destructively and this could be considered heat rather than seismic energy. The technique presented here is thought to be more robust and yields more realistic event magnitudes.

2.2.4. Multiple crack events

If each microcrack (bond breakage) is considered a single seismic event, then almost all of the recorded events exhibit similar magnitudes. This is not a realistic situation since it is known that earthquake magnitudes generally exhibit a power law distribution (Gutenberg and Richter, 1954). It is therefore postulated that in PFC, microcracks (bond breakages) occurring close together in space and time may be part of the same macro-rupturing event. This is probably a realistic assumption as it is known that most seismic events in the field are made up of many smaller scale ruptures and shearing of asperities (Scholz, 1990) and that fractures generally grow at some finite velocity (Madariaga, 1976).

For each microcrack in PFC, the forces surrounding the source particles are monitored for a specified length of time. The duration of the event is determined by assuming that a fracture propagates at half the shear wave velocity of the rock (Madariaga, 1976). The moment tensor is calculated each step from the

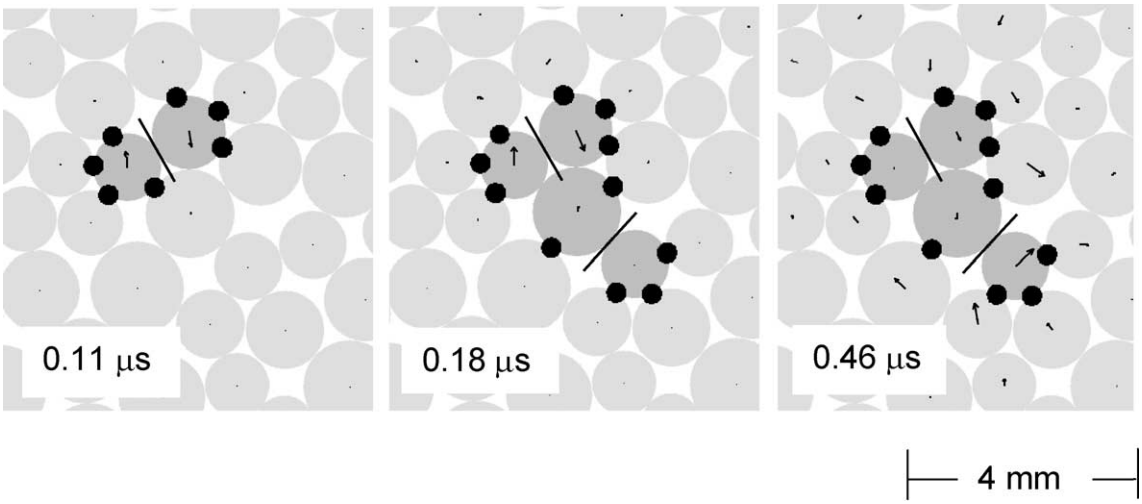

Fig. 3. Evolution of an event composed of two shear microcracks. The contacts surrounding the source are indicated by small black circles. Times given are from the time of the first bond breakage.

time of bond breakage to twice the time it would take a shear wave to propagate to the edge of the source area (one particle diameter). If another crack forms adjacent to the active crack such that the source areas overlap, the cracks are considered part of the same event, the source surface is reformulated and time is set back to zero. In this way, events made up of multiple cracks can exist and more realistic magnitude distributions result. This also means that a fracture propagating across the rock model would be considered a single seismic event, as would be the case if waveforms were recorded and seismic source information was calculated through waveform inversion. Fig. 3 shows an example event composed of two bond breakages. This technique is the same as that used in Hazzard and Young (2000) except that the technique presented here is more rigorous in that the source area is assumed to be only the two particles adjacent to the crack rather than an area of some arbitrary size.

3. Example application

3.1. General considerations

To test the modelling technique, an actual field experiment was simulated in which seismic data were recorded. It was thought that the seismic source information calculated from the model could be compared with the seismicity recorded in the field. If the comparison were favourable, this would give confidence in the validity of the model and the moment tensor calculation techniques.

The field experiment chosen for simulation was a well-controlled tunnel excavation with extensive seismic monitoring (the mine-by tunnel experiment). The host rock at the site is homogeneous and brittle and the seismic data quality is excellent. Mechanical and seismic data are plentiful thereby providing an excellent test-bed for the modelling techniques. In addition, static modelling of the tunnel excavation has already been attempted using PFC and results from this modelling have been positive. As well as providing a means for model validation, this particular excavation was simulated to try to help better understand the micromechanics of deformation that lead to the observed seismicity. The model is used to examine the time dependence of the seismic sources using the techniques described in Section 2.2.3 and the mechanics of the sources are examined directly by observing the particle motions over the duration of the events.

3.2. The mine-by tunnel

The mine-by tunnel is a 3.5-m diameter circular tunnel excavated in massive Lac du Bonnet granite

450 m below the surface in Manitoba, Canada. The tunnel is part of Atomic Energy of Canada Limited's (AECL) Underground Research Laboratory (URL) and is part of a large experiment to assess the feasibility of nuclear waste disposal in granite batholiths (see Read and Chandler, 1999 for details). The tunnel was excavated to experience the largest possible stress differential to try to produce a worst-case scenario in terms of rock stability. The maximum stress at the site is 60 MPa subhorizontal and the minimum stress is 11 MPa subvertical. The high stress differential caused cracking and spalling in the roof and floor of the tunnel and eventual notch formation—similar to a borehole breakout observed in the petroleum industry.

During the tunnel excavation, the seismicity was monitored by an array of 16 triaxial accelerometers. The frequency range of the sensors was 0.5–10 kHz meaning that events with moment magnitudes down to −4 could be detected. Approximately 10,000 events were recorded during and after the 46-m tunnel excavation (see Collins and Young, 2000 for details). Since a 2D model is being generated, only a narrow slice of the tunnel will be considered. Seismic data were analysed in detail for a 1.3-m section of the mine-by tunnel known as Round 7 (Collins, 1997). Ninety-eight events were located in the Round 7 volume (see Fig. 4). Of these, 62 were actually recorded ahead of the face before the Round 7 excavation. Because of the inability to consider 3D effects in the model, only the 36 events occurring after the Round 7 excavation will be considered here. Of these 36 events, 29 produced locations and 20 produced high-quality moment tensors. All of the events occurred within 2 months of the excavation. Note that as these events were occurring, the tunnel excavation continued until the tunnel extended a significant distance away from the Round 7 volume (see Fig. 4). There is clearly an important 3D effect causing stress changes and rotations as the tunnel passes by the region of interest (see Eberhardt, 2001). However, it can be shown that in this case, the maximum stress in the roof of the tunnel does not surpass the stresses calculated in the two-dimensional solution and that the rotations in principal stress directions are minimal. It will be assumed that a 2D representation is reasonably accurate, however, it is clear that some effects (e.g. rock degradation ahead of the face) can only be considered with a 3D model.

Table 1
Microparameters used in the PFC model of Lac du Bonnet granite

Microparameter	Value
Contact Young's modulus (GPa)	62
Ratio of contact normal stiffness to shear stiffness	2.5
Interparticle friction	0.5
Average bond tensile strength (MPa)	157
Standard deviation in bond tensile strengths (MPa)	36
Average bond shear strength (MPa)	157
Standard deviation in bond shear strengths (MPa)	36

Table 2
Model macro properties obtained from simulated axial compression tests on modelled core samples compared with data from actual tests on Lac du Bonnet granite

Property	Model value	LdB granite value
Young's modulus (GPa)	71	69
Poisson's ratio	0.24	0.26
Unconfined compressive strength (MPa)	199	200

Granite data are from Martin (1993).

Fig. 5 shows the source types for the 20 events in the Round 7 volume (note that the event that appears to be occurring inside the tunnel is mislocated). It appears that the majority of these events show a predominantly implosive source mechanism. This agrees with moment tensor solutions obtained for other excavation rounds in the same tunnel (Feignier and Young, 1992, 1993). Closure of preexisting cracks due to rotating stress fields was thought to be the mechanism by which these implosions could have occurred. However, there is still some doubt as to the exact mechanisms, especially since physical observations clearly show extensile opening and slabbing in the notch region (see Fig. 6).

It was thought that micromechanical models as described here could help resolve this ambiguity. If a model was created that reproduced the observed seismic results, this would give confidence that the model was behaving in a realistic manner. The model

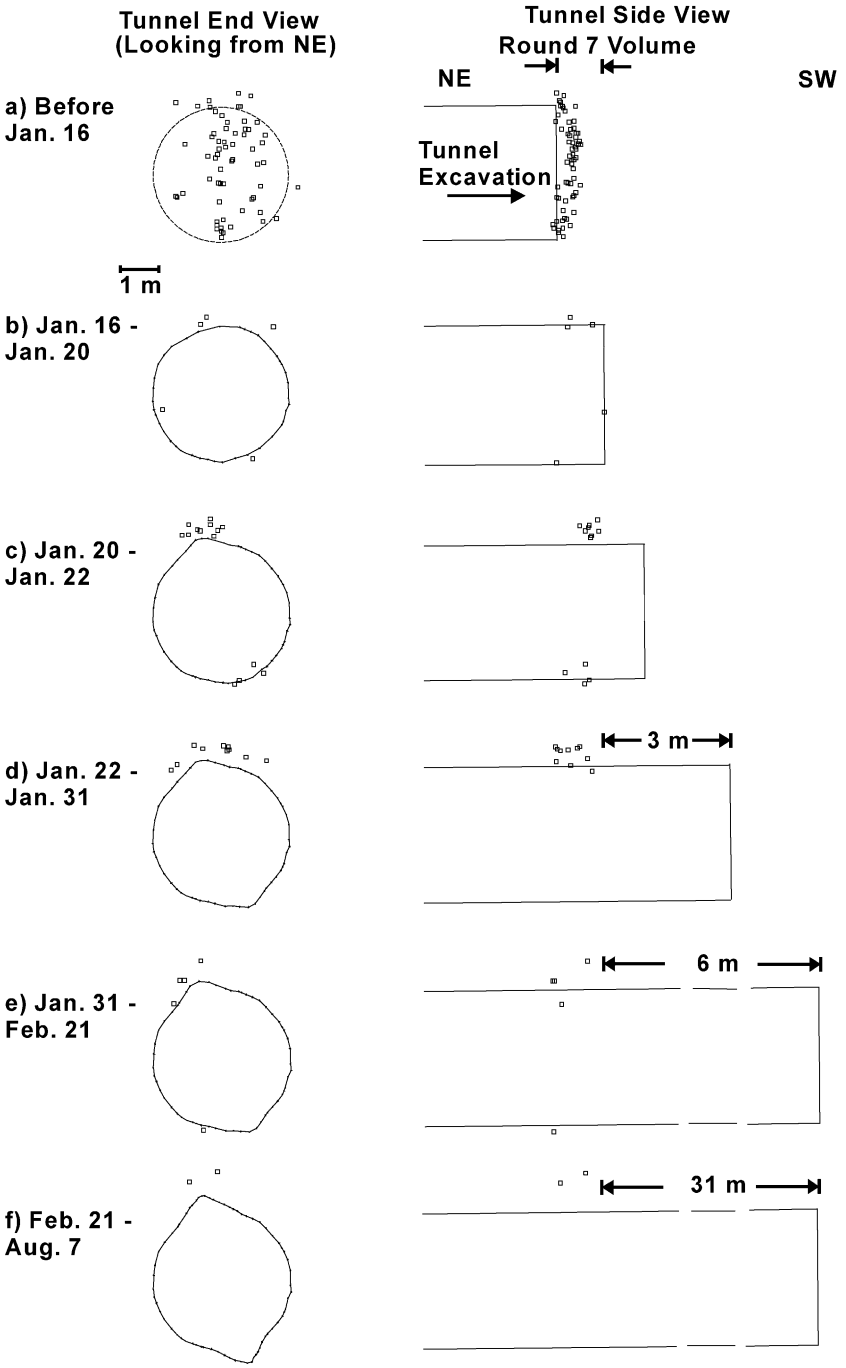

Fig. 4. Locations of all events recorded in the Round 7 volume (from Collins, 1997).

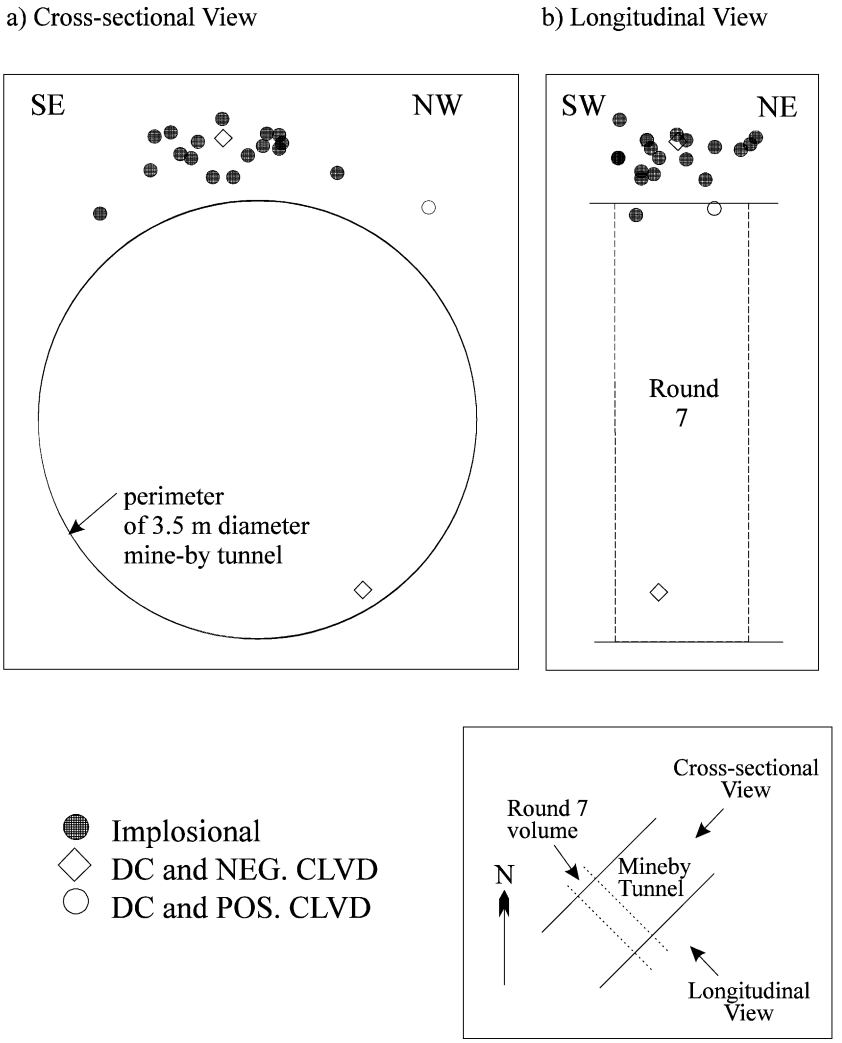

Fig. 5. Source mechanisms of 20 events recorded after a 1-m excavation round. Filled symbols represent predominantly implosive events whilst open symbols represent predominantly deviatoric events. Reproduced from Collins (1997).

could then be used to examine the micromechanics of cracking and failure in the notch region to try to better explain the seismic and physical observations.

3.3. The model

A sophisticated static PFC model of the mine-by tunnel notch region has been created by Itasca Consulting Group to try to explain the mechanics behind the observed damage (see Chandler et al., 2000). It is not the intention of this paper to describe in detail the implementation of this model. Instead, we wish to run the model dynamically to test the moment tensor calculation techniques and to show how seismic information can be extracted from the model and compared with actual recorded seismicity. Therefore, only a brief description of the static model will be given here.

Before the tunnel model was created, the microparameters required to reproduce the behaviour of Lac du Bonnet granite were determined by running simulations of axial compression tests on core samples. The microparameters in the models were adjusted until the models reproduced the strength, stiffness

Fig. 6. Photograph of lower notch, exposed by excavating a trench in the floor.

and Poisson's ratio of actual Lac du Bonnet granite. Table 1 shows the model microparameters used and Table 2 shows the resulting model macro behaviour compared to the mechanical behaviour of actual Lac du Bonnet granite core samples.

These parameters were then used to generate a model of the tunnel. A 2D section of the tunnel was simulated by a coupling of continuum and PFC models. Since the actual tunnel is 46 m long, it was assumed that in the centre of the tunnel the end effects would be negligible and a 2D model could accurately represent the stress situation (this is not strictly true because there are 3D effects as the tunnel is excavated past the area of interest—see Section 3.2). The notch region was modelled by an assemblage of PFC particles and this was then coupled to a continuum code (FLAC—Itasca Consulting Group, 2000). This allowed for high-resolution representation of the region of interest (see Fig. 7).

When the tunnel excavation was simulated, it was found that very little cracking occurred in the model. It was thought that some time-dependent mechanism was likely responsible for the damage and failure in the actual tunnel, so a stress-corrosion algorithm was written into the model to try to simulate the time-dependent effect. This algorithm basically weakens the interparticle bonds with the amount of weakening dependent on the stress at the contact and the length of time that the bond has been subjected to the stress. The algorithm was calibrated by simulating laboratory static fatigue tests in which core samples were held at different levels of stress until failure. For more details of the stress-corrosion algorithm, see Potyondy and Cundall (1998).

When the stress-corrosion algorithm was activated, the crack locations in the model delineated a region of approximately the same size and shape as the actual observed notch. This provided confidence that the model was behaving in a realistic manner. However, it was thought that the model could be further validated by comparing the seismicity generated by the model to actual recorded seismicity.

3.4. Seismicity

The static model described in Section 3.3 was run with high levels of numerical damping so that energy released from bond breakages would be quickly removed and a state of static stress equilibrium would be reached. To extract seismic information from the model, realistic levels of damping need to be specified so that realistic attenuation of seismic waves can occur. Feustel (1995) calculated the P-wave seismic quality factor, Q, at the URL to be approximately 200. This value was used to calculate the numerical damping required in the model using the technique described by Hazzard et al. (2000). By specifying a low level of numerical damping, strain energy released from the particle contacts after bond breakage can be partially converted into kinetic energy (seismic waves) and seismic source information can be calculated. The model described in Section 3.3 was therefore rerun with this low value of numerical damping and with the seismic monitoring algorithms in place.

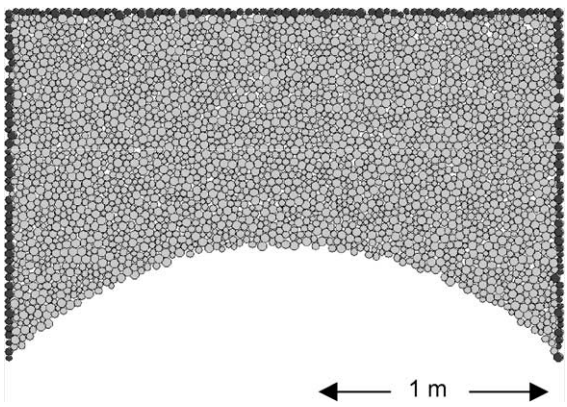

Fig. 7. PFC^{2D} portion of the mine-by model (3051 particles). Boundary particles that link to continuum model are darkened.

3.5. Results and interpretation

3.5.1. Locations and magnitudes

The tunnel excavation was simulated and stress corrosion was applied to simulate time-dependent deformation in the notch region. Because the model is only two-dimensional, it was assumed that the model represented only a 2D slice of the tunnel excavation. The model results are therefore compared only to actual seismicity occurring within a 1.3 m slice (Round 7) as described in Section 3.2.

The PFC model was run for a simulated 4 years, however, a clear drop in the rate of seismicity occurred after 55 days. This period of time is similar to the period of time in which seismicity was recorded in the tunnel after the Round 7 excavation (49 days). Therefore, only modelled seismicity occurring within the first 55 days will be examined here. During this time, 235 seismic events were 'recorded' in the model. Note that 345 bond breakages occurred, therefore many of the events were composed of several individual microcracks. Moment tensors and magnitudes were calculated for each of the events using the techniques described in Section 2.2. Fig. 8 shows the temporal and spatial distribution of the modelled events compared with actual seismicity recorded in the field experiment. The events are coloured according to time and the circle sizes are proportional to the event magnitudes. Note that the PFC model generates many more events than were actually recorded and that this has necessitated reducing the size of the PFC events in Fig. 8 for ease of viewing.

It is clear in Fig. 8 that the model reproduces the spatial pattern of the seismicity. The PFC events seem to delineate the zone of damage (the notch) as do the recorded events. Note that the actual seismicity is possibly being located too far from the tunnel due to path effects caused by the tunnel. The mean error in event location for these events is 26 cm and the maximum error is 45 cm. It is likely that if more accurate locations were obtained, then the two plots in Fig. 8 would be even more similar.

The temporal patterns exhibited by the modelled and recorded events also show similarities. Both the

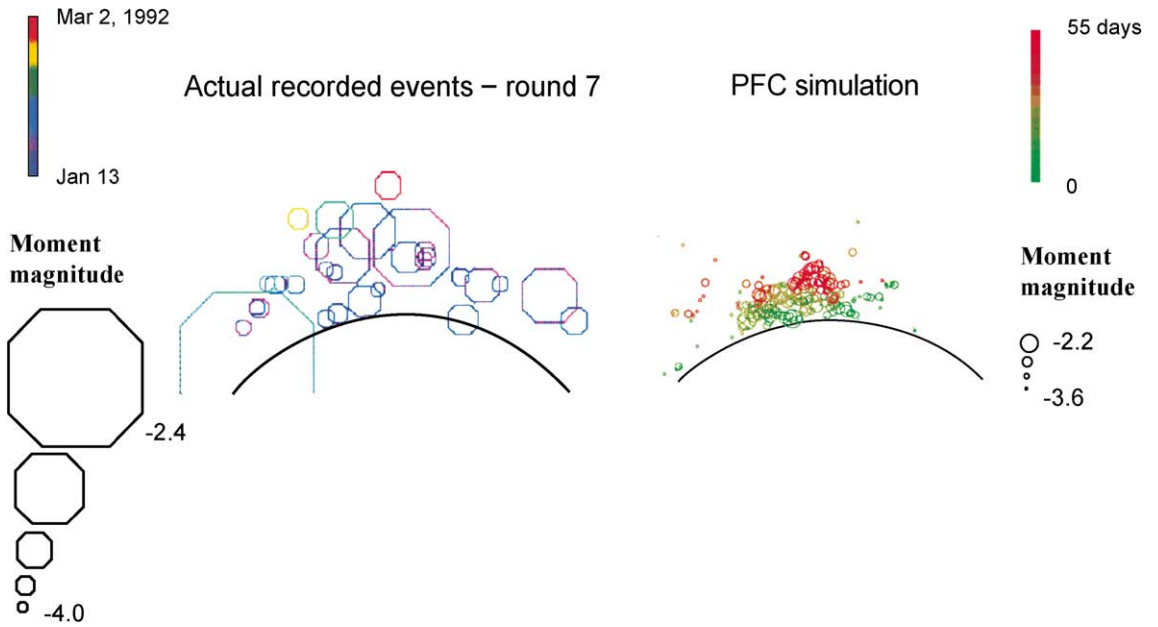

Fig. 8. Seismic events generated by the PFC model compared with actual recorded events occurring after a 1-m excavation round (Round 7). Events are coloured according to time and scaled according to moment magnitude. The plot showing the actual seismic data is adapted from Collins (1997).

model and the actual data show that seismicity starts near the tunnel edge and migrates into the rock over the 2 months following the excavation.

Finally, the moment magnitudes calculated for the PFC events and for the recorded seismicity are very similar. The moment magnitude is a measure of the strength of an event and the ability of the model to accurately reproduce the magnitudes observed during notch formation gives confidence that the model is producing similar-sized episodes of deformation as occurred in reality.

There are some discrepancies between the model and field magnitudes. Firstly, it appears that the range in event magnitudes produced by the model is too narrow. This can be observed quantitatively by calculating the seismic *b* value. The seismic *b* value is a measure of the distribution of magnitudes (see Gutenberg and Richter, 1954) and generally has a value close to one for earthquake sequences occurring in nature. When this calculation is performed for the 235 events produced by the model, a *b* value of 3.8 results. This is significantly greater than the expected value close to unity and is also greater than the value of 1.6 calculated for the actual events recorded above the 1-m tunnel excavation. It is clear therefore that the magnitude distribution of the PFC generated events is much too narrow. The reason for this is not totally clear but it is suspected that because the model is 2D there are fewer crack interactions than there would be in 3D and therefore there are fewer large magnitude events. Work is currently being done to expand the modelling techniques to three dimensions and preliminary results show that *b* values produced by these 3D models are generally less than 2. More study is needed on this topic.

Table 3
Event types observed during the PFC mine-by simulation compared with event types calculated from actual recorded seismicity at the mine-by (Round 7)

Dominant mechanism	Percentage (%) of total PFC-generated events ($N=235$)	Percentage (%) of total recorded events ($N=20$)
Explosive	51	0
Implosive	23	85
Deviatoric	26	15

Mine-by data from Collins (1997).

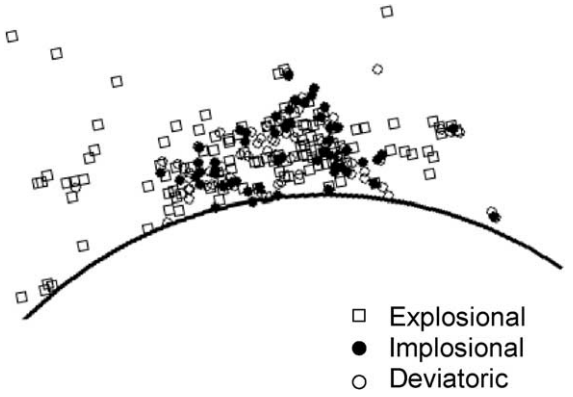

Fig. 9. Source mechanisms calculated from the moment tensors for the modelled events.

Another discrepancy between the model and the experiment is that the events produced by the model exhibit magnitudes that are slightly too large. The magnitudes in the model could be decreased by introducing a contact softening law that allows the bonds to break gradually over some finite time instead of instantly (see Huang et al., 1999). This has not yet been attempted.

3.5.2. Moment tensors

To examine the nature of the sources, moment tensors were decomposed into isotropic and deviatoric components by the method described in Feignier and Young (1992). These results are displayed in Table 3 and are shown graphically in Fig. 9.

In the PFC simulation, more than half of the events are predominantly explosive. This agrees with physical observations of the notch that show fractures opening perpendicular to the tunnel surface (Fig. 6). Fig. 10 shows the moment tensors (plotted as principal forces) for the events occurring within the first 30 h of the simulated excavation. It seems clear from this figure that the majority of the events are explosive and that the principal direction of opening (tension) is subperpendicular to the tunnel surface.

Interestingly, Fig. 9 and Table 3 indicate that about a quarter of the events exhibit a predominantly *implosional* mechanism. This is interesting because an implosional mechanism seems counterintuitive when observing Fig. 6, however, the majority of events actually recorded in the notch region were predominantly implosive. Fig. 5 shows the mechanisms of the

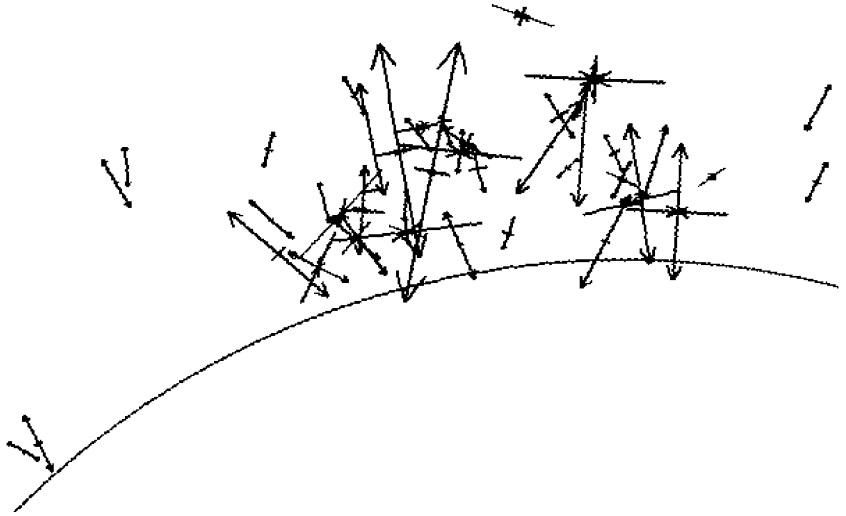

Fig. 10. Moment tensors for events occurring within 30 h of the simulated excavation.

20 events recorded after the excavation of Round 7 for which accurate moment tensors could be calculated.

Fig. 10 shows that the direction of implosion (pressure) for the modelled events is generally sub-parallel to the tunnel surface. To try to better understand the mechanics of these implosive events, several were examined in detail by observing the motions of particles over the duration of the event. One example is shown in Fig. 11. This figure shows how an implosive event evolves through time. The event is composed of several tensile microcracks oriented parallel to the surface of the tunnel. The cracks are initially opening perpendicular to the tunnel surface and this is reflected in the calculated moment tensor for the event. As time progresses, particles continue to move perpendicular to the tunnel surface, but particles to the left and right of the event begin to push inwards to compensate for the volume change. The moment tensor then begins to look more deviatoric. Finally, at the time of peak scalar moment, the compressive component acting parallel to the tunnel surpasses the explosive component and the moment tensor displays a predominantly implosive mechanism. Note that at this time, particles are still moving rapidly into the tunnel void, however, this does not contribute much to the moment tensor calculation because the particles moving into the tunnel are not pushing against other particles (no contacts are being deformed).

3.5.3. Errors

For the seismicity recorded in the field, three quality indices were calculated for each event: one related to the data quality, one related to the sensor coverage and one related to the goodness of fit between the radiation patterns calculated from the moment tensor model and the actual observed values (see Mendecki, 1993). The quality indices range from 0 to 1. Of the 36 events recorded after the Round 7 excavation, 20 produced moment tensors with each of the three quality factors greater than 0.6. Only these 20 events are presented here therefore it can be assumed that these mechanisms are reliable.

It is difficult to estimate errors for the PFC generated moment tensors since there are no waveform amplitudes that can be compared to a proposed model, however, a rough error estimate was made by looking at the difference between the two off-diagonal components of the moment tensor, M_{12} and M_{21}. Conservation of angular momentum states that the moment tensor should be symmetric (Gilbert, 1970), therefore, the difference in the two off-diagonal components should give some estimate of the error. It was found that in general, the two components differed by a factor of 2 or less, although some events showed very large differences (up to an order of magnitude). The importance of these errors was assessed by decomposing the moment tensor using the M_{12} value

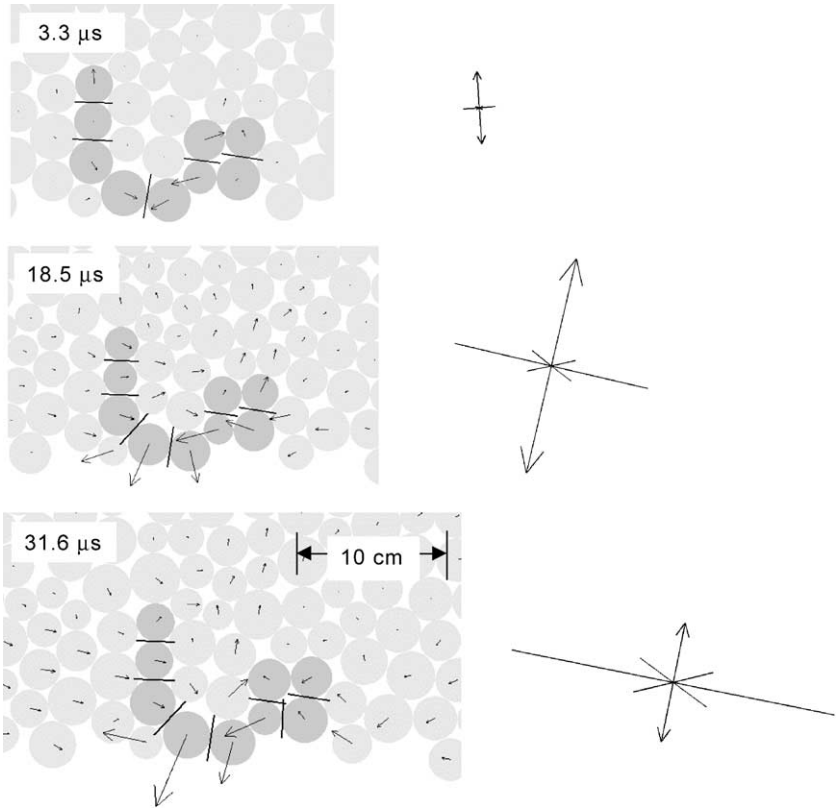

Fig. 11. The evolution of a large implosive event. Source particles are darkened. Particle velocities are shown by arrows. Black lines show microcrack locations. Moment tensors calculated at each time are shown to the right. The bottom image corresponds to the time of maximum scalar moment.

in both off-diagonal matrix positions and then using the M_{21} value in both positions. Of the 235 events, 97% displayed less than a 10% difference in the calculated isotropic component and 50% displayed less than a 2% difference. It is assumed therefore that the interpretations presented are assumed to be valid. In all of the analyses presented above, the average of M_{12} and M_{21} is used in the calculations.

The reasons for this observed difference in M_{12} and M_{21} are not entirely clear. There appears to be no relationship between the error and the event magnitude, location, or the number of individual microcracks involved. It is suspected that the errors arise because the moment tensor is calculated at a single point in time and that angular momentum is only conserved if particle motions over the whole duration of the event are considered. More investigation of this topic is required.

3.5.4. Interpretation

The PFC model reproduces quantitatively the spatial and temporal distribution of the observed seismicity and the moment magnitudes of the events. There are a few small discrepancies, the most important of which is that the *b* value of the modelled events is too large. However, the similarities between the model and the field results are encouraging and give confidence that the model is behaving in a realistic manner.

The calculated event mechanisms appear intuitively realistic as well even though quantitative comparisons cannot really be made due to the 2D nature of the model. One clear discrepancy between the model and the actual data is the presence of many explosional events in the model that are not observed in the seismic data. It is possible that these tensile events may actually be occurring in the rock but that they are

not recorded. This idea is supported by physical observation that shows fractures opening perpendicular to the tunnel surface. A possible explanation for this is that the tensile events may not be releasing enough energy (or they may radiate frequencies that are too high) to be detected by the seismic sensors. When high-frequency acoustic emission monitoring was performed in a small rock volume in the sidewall of the tunnel (tensional stress regime), many events were recorded that were not picked up by the lower-frequency microseismic system (Carlson and Young, 1993). In the numerical model, *all* events are 'recorded' regardless of magnitude or frequency. The modelled events were examined to see if the shear and implosive events were significantly larger than the tensile events, however, this was found not to be the case. One of the reasons for this may be that the tensile bond strengths are unrealistically high relative to the shear bond strengths (see Table 1). It is possible that if lower tensile bond strengths were assigned, then the tensile events would be smaller. This has not yet been attempted.

There may be other factors contributing to the lack of recorded tensile events that have little to do with the actual mechanics. For example, Šílený et al. (2001) show that spurious non-double couple components can appear in the source mechanism if the effects of the tunnel are ignored in the inversion. These effects have not been considered in the analyses presented here.

Even though this discrepancy in mechanisms exists, the model can still be used to examine the micromechanics of failure. For example, many unexpected implosive events are observed in the model and in the field and the model can be used to help explain the mechanics behind them. An example modelled implosive event is shown and the mechanism is explained by examining the time dependence of the source. It was found that the implosive sources initially show tensile motion perpendicular to the tunnel, but then compressive motion occurs parallel to the tunnel to compensate for the volume change. This mechanism seems plausible, especially when it can be observed that much buckling of slabs occurs in the notch region (see Fig. 6). This example highlights the importance of trying to understand how source mechanisms can evolve through time—possibly changing from tension to compression within the same event. Baker and Young (1997) use a time-dependent moment tensor inversion technique to show that events at the mine-by tunnel often show an initial tensile component and then evolve into shear-type events over the rupture history. Further investigations of this type may assist in the interpretations.

Clearly, the PFC model is a simplification of what occurs in reality. For example, no consideration is made of the three-dimensional effect caused by the advancing tunnel. It is likely that rock degradation will occur ahead of the face and that stress changes and rotations will occur as the tunnel passes by. Another simplification is the use of round grains to simulate a crystalline rock. The model could be made more realistic by clustering groups of particles into grains of different angular shapes (Boutt and McPherson, 2002). This has not yet been attempted. However, even with these simplifications, it has been shown that the model can provide useful insights into possible mechanisms occurring during rock fracture and failure.

4. Discussion and conclusions

This study outlines how micromechanical modelling can be used to simulate seismicity and describes a possible technique for determination of seismic source information (magnitudes and moment tensors) for the synthetic earthquakes. The modelling is unique in that no a priori assumptions are made about the nature of the source before the simulation. In this way, not only shear-type events can be simulated, but events containing significant isotropic components are also observed. This is especially important when trying to simulate induced seismicity (e.g. mining) where non-double couple events are common.

The ability to extract and quantify seismic source information from the models presents a useful way to validate the model behaviour. As well as stress/strain behaviour and observations of the damage incurred in the models, comparing seismic locations, magnitudes and mechanisms to results obtained from actual recorded seismic data can give further confidence that the models are behaving in a realistic manner. Once this has been ascertained, the models can be used to examine the possible micromechanics of the failure and to help explain the nature of deformation that is causing the observed seismicity. The modelling tech-

nique is tested by simulating notch formation at the edge of a highly stressed tunnel. It was found that the model generated many implosional events agreeing partially with the actual recorded seismicity. It was then shown how the model could be used to enhance the interpretation of these events by examining the micromechanics and the time dependence of the deformation directly. It was shown that in the model, the implosive events actually initiated as tensile cracks but evolved into implosional regimes as volume compensation occurred.

Obviously, this is only one possible explanation and the models are clearly still a large simplification of what occurs in reality. In particular, the model is only two-dimensional and the micromechanics are greatly simplified. In theory, these simplifications can be partially overcome, however, in practice, the jump in processing power required for 3D models of equivalent resolution is enormous. To try and overcome this, a new project is being undertaken to allow intelligent switching between continuum and discontinuum components within the model and to use massive parallel computers.

Other modifications could be made to improve the match between the model and the observed results, for example, introducing a larger range in grain sizes, bonding together grains into more angular shapes, or including a contact softening law. These modifications are planned for the future, however, this study has highlighted how even with a fairly simple model, seismic information can be extracted and model verification can be performed by comparing the modelled seismicity to the nature of the seismicity recorded in the field. This study also shows an example of how the models could then be used with more confidence to examine in detail the nature of damage and failure in rocks.

Acknowledgements

The authors wish to thank the Engineering and Physical Sciences Research Council UK (EPSRC/DTI LINK Oil and Gas Extraction Programme Project No. 8066) and Atomic Energy of Canada for funding this research. We also wish to thank David Bowers at Atomic Weapons Establishment, Blacknest for his help in formulating the moment tensor calculation procedure and David Collins for permission to reproduce some of his figures. A further acknowledgement goes to David Potyondy and Peter Cundall at Itasca Consulting Group for the use of their model and advice in all aspects of the modelling. An acknowledgement goes to the two reviewers and volume editor whose comments have greatly improved this paper.

References

Aki, K., Richards, P.G., 1980. Quantitative Seismology. Freeman, New York, 932 pp.

Antonellini, M.A., Pollard, D.D., 1995. Distinct element modeling of deformation bands in sandstone. Journal of Structural Geology 17, 1165–1182.

Backus, G.E., 1977. Interpreting the seismic glut moments of total degree two or less. Geophysical Journal of the Royal Astronomical Society 51, 1–25.

Baker, C., Young, R.P., 1997. Evidence for extensile crack initiation in point source time-dependent moment tensor solutions. Bulletin of the Seismological Society of America 87 (6), 1442–1453.

Boutt, D.F., McPherson, B.J.O.L., 2002. Simulation of sedimentary rock deformation: lab-scale model calibration and parameterization. Geophysical Research Letters 29 (4), 13.1–13.4.

Bowers, D., Hudson, J.A., 1999. Defining the scalar moment of a seismic source with a general moment tensor. Bulletin of the Seismological Society of America 89 (5), 1390–1394.

Carlson, S.R., Young, R.P., 1993. Acoustic-emission and ultrasonic velocity study of excavation-induced microcrack damage at the underground research laboratory. International Journal of Rock Mechanics and Mining Sciences and Geomechanics Abstracts 30 (7), 901–907.

Chandler, N., Read, R., Cundall, P., Potyondy, D., Detournay, E., Young, R.P., Lau, J.S.O., 2000. An integrated approach to excavation design—a project within Canada's used fuel disposal program. In: Girard, J., Liebman, M., Breeds, C., Doe, T. (Eds.), Rock Around the Rim: Proceedings of the 4th North American Rock Mechanics Symposium. Balkema, Seattle, pp. 1271–1278.

Collins, D.S., 1997. Excavation Induced Seismicity in Granitic Rock: A Case Study at the Underground Research Laboratory, Canada. Keele University, Staffordshire, UK, 256 pp.

Collins, D.S., Young, R.P., 2000. Lithological controls on seismicity in granitic rocks. Bulletin of the Seismological Society of America 90 (3), 709–723.

Cundall, P.A., Strack, O., 1979. A discrete element model for granular assemblies. Geotechnique 29, 47–65.

Eberhardt, E., 2001. Numerical modelling of three-dimension stress rotation ahead of an advancing tunnel face. International Journal of Rock Mechanics and Mining Sciences 38 (4), 499–518.

Feignier, B., Young, R.P., 1992. Moment tensor inversion of induced microseismic events—evidence of nonshear failures in the $-4 < M < -2$ moment magnitude range. Geophysical Research Letters 19 (14), 1503–1506.

Feignier, B., Young, R.P., 1993. Failure mechanisms of microseismic events generated by a breakout development around an underground opening. Rockbursts and Seismicity in Mines 93, 181–186.

Feustel, A.J., 1995. Seismic Attenuation in Underground Mines: Measurement Techniques and Applications to Site Characterization. Queen's University, Kingston, Ontario, Canada, 193 pp.

Gilbert, F., 1970. Excitation of the normal modes of the earth by earthquake sources. Geophysical Journal of the Royal Astronomical Society 77, 883–914.

Gutenberg, B., Richter, C.F., 1954. Seismicity of the Earth and Associated Phenomena. Princetown Univ. Press, Princetown.

Hanks, T.C., Kanamori, H., 1979. A moment magnitude scale. Journal of Geophysical Research 84, 2348–2350.

Hazzard, J.F., Young, R.P., 2000. Simulating acoustic emissions in bonded-particle models of rock. International Journal of Rock Mechanics and Mining Sciences 37 (5), 867–872.

Hazzard, J.F., Young, R.P., Maxwell, S.C., 2000. Micromechanical modeling of cracking and failure in brittle rocks. Journal of Geophysical Research—Solid Earth 105 (B7), 16683–16697.

Huang, H.Y., Detournay, E., Bellier, B., 1999. Discrete element modelling of rock cutting. Rock Mechanics for Industry, vols. 1–2. Balkema, Rotterdam, pp. 123–130.

Itasca Consulting Group, 1999. PFC2D (Particle Flow Code in 2 Dimensions). Itasca Consulting Group, Minneapolis, MN.

Itasca Consulting Group, 2000. FLAC (Fast Lagrangian Analysis of Continua). Itasca Consulting Group, Minneapolis, MN.

Madariaga, R., 1976. Dynamics of an expanding circular fault. Bulletin of the Seismological Society of America 66, 639–666.

Martin, C.D., 1993. Strength of Massive Lac du Bonnet Granite Around Underground Openings. University of Manitoba, Winnipeg, Manitoba.

McGarr, A., 1994. Some comparisons between mining-induced and laboratory earthquakes. Pure and Applied Geophysics 142, 467–489.

Mendecki, A.J., 1993. Real time quantitative seismology in mines. In: Young, R.P. (Ed.), Rockbursts and Seismicity in Mines. Balkema, Kingston, Ontario, Canada, pp. 287–296.

Mora, P., Place, D., 1998. Numerical simulation of earthquake faults with gouge: toward a comprehensive explanation for the heat flow paradox. Journal of Geophysical Research 103, 21067–21089.

Morgan, J.K., Boettcher, M.S., 1999. Numerical simulations of granular shear zones using the distinct element method: 1. Shear zone kinematics and the micromechanics of localization. Journal of Geophysical Research—Solid Earth 104 (B2), 2703–2719.

Potyondy, D., Autio, J., 2001. Bonded-particle simulations of the in-situ failure test at Olkiluoto. In: Elsworth, D., Tinucci, J.P., Heasley, K.A. (Eds.), Rock Mechanics in the National Interest: Proceedings of the 38th U.S. Rock Mechanics Symposium. Balkema, Washington, DC, pp. 1553–1560.

Potyondy, D., Cundall, P., 1998. Modeling notch-formation mechanisms in the URL mine-by test tunnel using bonded assemblies of circular particles. International Journal of Rock Mechanics and Mining Sciences 35 (Paper No. 067).

Potyondy, D.O., Cundall, P.A., Lee, C.A., 1996. Modelling rock using bonded assemblies of circular particles. In: Aubertin, M., Hassani, F., Mitri, H. (Eds.), Rock Mechanics Tools and Techniques, Proceedings of the Second North American Rock Mechanics Symposium. Balkema, Montreal, pp. 1937–1944.

Read, R., Chandler, N., 1999. Excavation damage and stability studies at the URL—rock mechanics considerations for nuclear fuel waste disposal in Canada. Rock mechanics for Industry: Proceedings of the 37th U.S. Rock Mechanics Symposium. Balkema, Vail, CO, pp. 861–868.

Scholz, C., 1990. The Mechanics of Earthquakes and Faulting. Cambridge Univ. Press, Cambridge, 439 pp.

Šílený, J., Pšencík, I., Young, R.P., 2001. Point-source inversion neglecting a nearby free surface: simulation of the underground research laboratory, Canada. Geophysical Journal International 146 (1), 171–180.

Silver, P.G., Jordan, T.H., 1982. Optimal estimation of scalar moment. Geophysical Journal of the Royal Astronomical Society 70, 755–787.